Charge transport model for disordered materials: Application to sensitized TiO_2

Juan A. Anta,[1] Jenny Nelson,[2] and N. Quirke[1]
[1]Department of Chemistry, Imperial College of Science, Technology and Medicine, South Kensington, SW7 2AY, United Kingdom
[2]Department of Physics, Imperial College of Science, Technology and Medicine, South Kensington, SW7 2AY, United Kingdom
(Received 30 April 2001; published 13 March 2002)

We propose a simple model of charge transport that predicts the conducting properties of disordered materials. The transport of charge is assumed to occur by trapping and detrapping of electrons in localized states and diffusion via a conduction-band level. The input is an arbitrary density of localized states (DOLS) and the output, bulk mobilities, and conductivities as a function of the field and the density of carriers. The code can be applied to any kind of carrier (electrons, holes, or ions) and includes trap-filling effects. This leads to predictions of density-dependent mobilities—a determining factor in the conducting properties of amorphous insulators and sensitized semiconductors. Using this model, we have studied the photoconductor TiO_2 by comparing the predicted conductivity for different DOLS with experimental data in steady-state conditions. Our simulations show that the presence of a few deep traps determines the observed superlinear dependence of the conductivity on the number density of carriers.

DOI: 10.1103/PhysRevB.65.125324 PACS number(s): 73.50.Gr, 73.50.Pz, 73.63.−b, 72.80.Ng

I. INTRODUCTION

The electrical properties of disordered insulators and semiconductors are of great interest both as a challenging set of fundamental problems and because of their technological applications. The electrical industry is interested in evaluating current-voltage characteristics of insulating materials[1,2] that are the key to the description of long-standing problems such as breakdown and aging processes in insulation for high-tension cables. Colloidal semiconductors such as TiO_2 and ZnO represent a new class of electronic materials with numerous technological applications, ranging from batteries and electrochromic devices to a new generation of solar cells based on dye-sensitized nanoparticulate films.[3–7] Semiconducting polymers[8,9] can be used as the emissive material in organic light-emitting diodes, and amorphous organic photoconductors used in xerography. In all these materials, the movement of charge (electrons, holes or ions) determines the electronic characteristics through a disordered medium, the nature of which is determined by the chemical composition and the microscopic structure of the material. A key objective for research on these materials has been the determination of carrier mobilities. Traditionally, mobilities are derived by interpreting measurements on photoinduced transient currents in terms of carrier activation out of traps.[10,11] In modeling such measurements, a broad analytic distribution of trapping energies (generally exponential or Gaussian) is often assumed. An important advance would be to use realistic density of localized states (DOLS) obtained either from *ab initio* calculations of the electronic structure or from spectroscopic measurements.

The case of sensitized wide-band-gap nanocrystalline metal-oxide films represent a very attractive class of materials for research.[6] They provide a model system for pure electron transport between localized states. In such materials electrons are injected into the porous semiconductor network by means of a sensitizer that absorbs light in the visible range of the spectrum. These electrons migrate within the network until they recombine with the surface or external electron acceptors (the process to be prevented in applications) or reach the collecting electrode. In the case of sensitized solar cells, the greater the fraction of photoinjected electrons that reaches the collecting electrode, the greater the efficiency of the cell.[7,14] Thus, electrons of *external* origin give rise to the transport of charge. There are no holes contributing to the conductivity unlike other photosensitive materials such as amorphous hydrogenated silicon.[12] Furthermore, electron transport in porous, nanocrystalline metal oxides exhibits a strong, nonlinear dependence on electron density and electron injection.[4,7,13–16] This observation is usually explained in terms of *trap filling*. The argument runs as follows: as more electrons are injected into a system with a distribution of trap energies, traps with larger energies with respect to the conduction-band level (*deep* traps) are progressively filled, leaving only shallow traps available for conduction. As the residence times of electrons in deep traps are much longer than those in shallow traps, the net mobility of the electrons is enhanced as the electron density increases. Nelson has recently reported simulations of electron transport in nanocrystalline TiO_2 electrodes.[17] The calculations considered several electrons simultaneously with the condition that only one electron is allowed per trap. The simulations demonstrated that the transient current decays faster with time when more electrons are used. To our knowledge, this is the first simulation study of charge transport that takes into account trap-filling effects. We note that the population of the trap states is a factor[7] that determines the kinetics of the recombination reaction between electrons and surface or electron acceptor oxidized species. Thus, an increase in the trap occupancy enhances the acceleration of charge recombination with injected electron density.

The study of the trap-filling effect in disordered TiO_2 provides an interesting link with other systems where nonlinear behavior of the conductivity is also observed. For instance, the case of trap-controlled conduction in insulating polymers.[1,2] In this case, the filling of traps is believed to have a significant effect on the current-voltage characteristics. The filling of the traps at higher voltages (strong injec-

 ©2002 The American Physical Society

tion) is considered to be related to the breakdown of the insulation.[1]

In all the cases mentioned above, charge transport can be described as the transfer of carriers between localized states or *traps* that act as potential wells for the moving carriers. The purpose of the present paper is to develop a general transport model that can be employed to describe *multiple-trapping* transport of charge in disordered media. Previous papers[18,19,25] have already addressed this kind of transport, both from the theoretical and the simulation point of view. However, much of this paper has been inspired by the description of "time-of-flight" experiments, i.e., these authors look at the problem of *transient currents* in thin films of fixed thickness. More generally, previous studies[20] are restricted to the case of single-particle simulations, where trap-filling effects are not taken into account. In the present paper we are interested in multiple-trapping transport of charge in *steady-state* conditions, in the *bulk* [three-dimensional (3D) size-independent calculations] and with explicit consideration of the effects of *trap filling*. All these factors must be taken into account if we aim to model, for instance, sensitized TiO_2 solar cells in real working conditions. Furthermore, we use nontrivial DOLS that correspond to known electron traps in the material under consideration. Hence, we pursue three main objectives in this paper: (1) the consideration of trap-filling effects, (2) generalization to size-independent (3D) calculations in the steady state, and (3) the use of nontrivial DOLS related to real experimental materials.

As mentioned above, for sensitized TiO_2 solar cells and many other applications, we are interested in the conducting properties of a material in the *bulk*, away from the electrodes. We wish to predict the mobility as a function of the field and the charge density so that this can subsequently be used in a macroscopic calculation that takes into account space-charge and electrode effects.[14,8] Hence, our simulation model applies *periodic boundary conditions* in the field direction (in contrast to some previous studies where the sample has a fixed width along the direction of the applied field[10,11]). We show that the predicted mobilities correspond to the infinite width limit of the finite-size calculations.

In a previous paper on nanocrystalline TiO_2, it has been demonstrated that an exponential DOLS with a characteristic temperature of ~800 K can fit experimental data for transient currents.[17] The localized, intraband states are thought to arise from surface defects associated with oxygen vacancies, that is, Ti^{3+} states and absorbed species. Nevertheless, little evidence could be obtained either in spectroscopic studies[21] or *ab initio* calculations[22] that the distribution of surface states should be exponential. In the present paper we try to reconcile the transport data with the information available regarding the energies of the surface traps in nanocrystalline TiO_2. Our simulations show that very small concentrations of very deep traps determine the density dependence of the conductivity and that it is these deep traps that should be the focus of further research.

The paper is organized as follows. In Sec. II, the simulation procedure and the model system are introduced and tested in ideal cases. In Sec. III we make use of the simulation to obtain photoconductivities in dye-sensitized nanocrystalline TiO_2 for several choices of the DOLS. Conclusions based on our simulations are presented in Sec. IV.

II. TRANSPORT MODEL

A. Basic description

We assume that transport of charge occurs by transfer of electrons between localized states or *traps*. In the simplest situation, all traps will have the same energy (i.e., a DOLS with the shape of a Dirac δ function). In this case, it can be shown that the mobility is given by[1,2,23]

$$\mu=\frac{2\nu_0 a}{lE}\exp\left(-\frac{\varepsilon}{kT}\right)\sinh\left(\frac{eEa}{2kT}\right), \tag{1}$$

where ν_0 is the attempt-to-jump frequency, a is the average distance between traps, l is the number of equivalent neighboring sites to which the carrier is allowed to jump,[23] E is the applied field, ε is the trap depth (activation energy), e is the elementary charge, k is the Boltzmann constant, and T is the absolute temperature. Although the original model was for ionic transport,[2] it can be used to describe conductivity of any kind of carrier[24] provided that there are no tunneling effects.

In the limit of very small fields ($eEa \ll kT$), Eq. (1) reduces to

$$\mu=\frac{\nu_0 a^2 e}{lkT}\exp\left(-\frac{\varepsilon}{kT}\right), \tag{2}$$

and in the absence of traps the mobility is given simply by

$$\mu=\frac{\nu_0 a^2 e}{lkT} \tag{3}$$

that corresponds to the mobility of a carrier performing a simple random walk with time step $t_0=1/\nu_0$ in a network of lattice constant a and coordination number l.

B. Computer simulation

Following Marshall[25] and Nelson,[17] we have implemented a random-walk simulation technique based on detrapping times between sites or traps. This method is related to but not the same as the so-called continuous-time random-walk model originally introduced by Scher and Montroll.[26] Our simulation runs as follows:

(1) A three-dimensional array of sites is set up.
(2) Each site is given *six* different *detrapping* times (to each one of its six nearest neighbors) according to its energy (see below).
(3) Carriers jump randomly from one site to a neighboring site.
(4) The carriers adopt the detrapping times of the sites they visit. The release times are then the difference between the detrapping times of the site and the time already spent by the carrier in that site.
(5) At each simulation step, the carrier having the *shortest* release time t_i is selected and allowed to jump. The re-

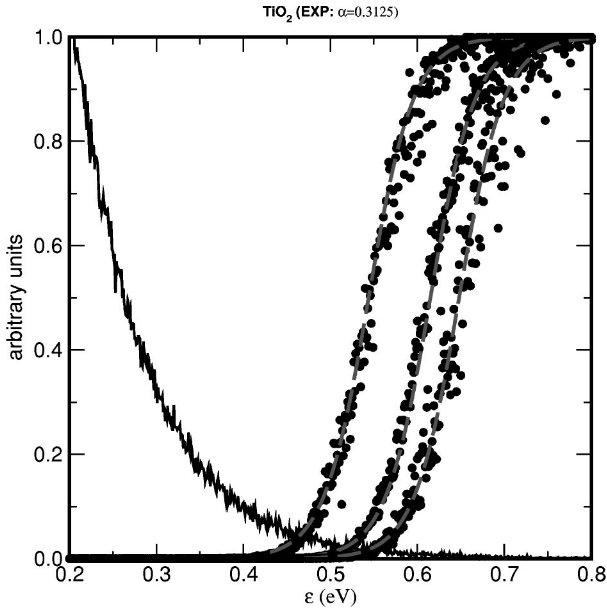

FIG. 1. Illustration of the trap-filling effect: probability that a trap of energy ε is occupied in an MTRW simulation (solid circles). Site energies are distributed according to an exponential density of states (solid line) with $\alpha = 0.3125$ [see Eqs. (7) and (8)]. The dashed lines correspond to fittings to a Fermi-Dirac distribution, $f(\varepsilon) = \{1+\exp[-(\varepsilon-\varepsilon_F)/kT]\}^{-1}$ (see Table I). The calculations were carried out for systems of ten particles in lattices of $18\times18\times18$, $24\times24\times24$ and $28\times28\times28$ sites, respectively (from left to right).

lease times of the rest of the carriers are then advanced by t_i. In the next step, the process is repeated.

The simulation method is an adaptive time-step procedure. This is important in the simulation of charge transport in disordered materials since detrapping times can vary by several orders of magnitude from site to site. Also, this procedure is particularly suitable if we want to monitor sudden increases of the mobility consequent on the filling of the deeper traps.

In the present paper we calculate the detrapping time between two sites i and j via the expression

$$t_{ij} = -\ln(r) t_0 \exp([\varepsilon_i + \mathbf{E}\cdot a\mathbf{u}_{ij}/2]/kT), \tag{4}$$

where r is a random number uniformly distributed between 0 and 1, t_0 is the minimum detrapping time, ε_i is the trap depth (energy) of the *starting* site i, $\mathbf{E}$ is the applied field, and u_{ij} is the unit vector linking sites i and j. The combination of exponential detrapping times with the additional requirement of single trap occupancy produces a Fermi-Dirac distribution for the probability of a trap being occupied at equilibrium at a temperature T (see Fig. 1).

In order for this algorithm to produce an equilibrium ensemble in the absence of an applied field, the condition of microscopic reversibility (sometimes called detailed balance[27]) must be obeyed. In our model the release rate from a site of energy ε_t is related to the capture rate by the ratio $\exp(\varepsilon_t/kT)$ (the probability of capture by an empty site is 1 in our model) and this ensures that, at equilibrium, the transition between states of the system occurs at the same rate.

In contrast to the papers of Marshal[25] and others, the present model does not contain a tunneling factor and motion is always between adjacent sites. These assumptions have been used successfully to model electron transport in TiO_2[17,28] and appear reasonable also for charge transport in polyethylene.[29] For systems with a wide distribution of trap energies, deep traps are in most cases surrounded by shallow traps so as to leave a deep trap that electron has to tunnel through an energy barrier almost equal to the trap energy (with respect to the conduction band). For such cases, even if tunneling occurs, the present model will give the correct qualitative behavior. Of course, neglect of tunneling will always be a good approximation as the temperature is increased.[30]

Equation (4) resembles a *multiple-trapping* mechanism of conduction:[31] carriers have to surmount an activation barrier to escape from one trap and move to an adjacent one. Thus, the detrapping time does not depend on the difference of energies between two sites[10] (as in hopping models) but on the activation energy of a single trap, i.e., a multiple-trapping random walk (MTRW). The logarithmic factor in Eq. (4) represents the random dispersion of detrapping times with respect to the mean detrapping time of the trap.[25,32]

As mentioned above, we aim to simulate conduction in the bulk and in the steady state. With this intent, we construct a three-dimensional lattice of sites whose energies are allocated by sampling the selected DOLS, and periodic boundary conditions are applied in all directions. During the simulation process, any carrier crossing one of the boundaries in the x direction (the direction of the applied field) is reinjected through the opposite side. The simulation is allowed to reach a stationary state (no variation with time of the current) and the current and the mobility are obtained from the number of carriers moving forward per unit time. The calculation is then repeated for several realizations of the DOLS. The mobilities are then extracted from

$$\mu = \frac{J}{e\rho E}, \tag{5}$$

where J is the current density, e is the charge of the carriers, and ρ is their density. By using this expression we neglect the polarization and diffusion components of the current density (once the stationary state is reached there is no density gradient). In the bulk calculation, J is obtained from counting the *net* number of carriers moving in the positive x direction in a selected *time window*. The result is then averaged, once the stationary state is reached, over several time windows (50, typically) and several realizations of the DOLS. The parameter t_0 [cf. Eq. (4)] controls the time scale of the simulation. It corresponds to the inverse of the attempt-to-jump frequency v_0 in Eq. (1).

C. One-particle simulations and finite-size effects

We have tested the MTRW code against the theoretical result, Eq. (1), which should hold for a one-particle simulation

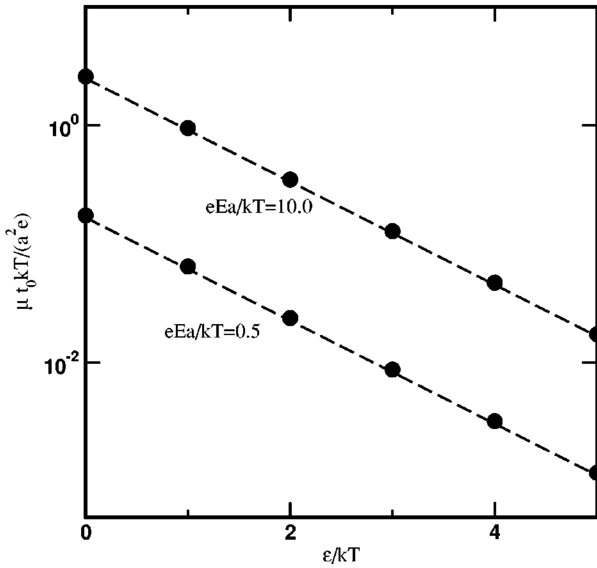

FIG. 2. Mobilities from Eq. (1) (dashed line) and from MTRW simulations in the bulk (circles) for different values of the trap energy ε and the electric field.

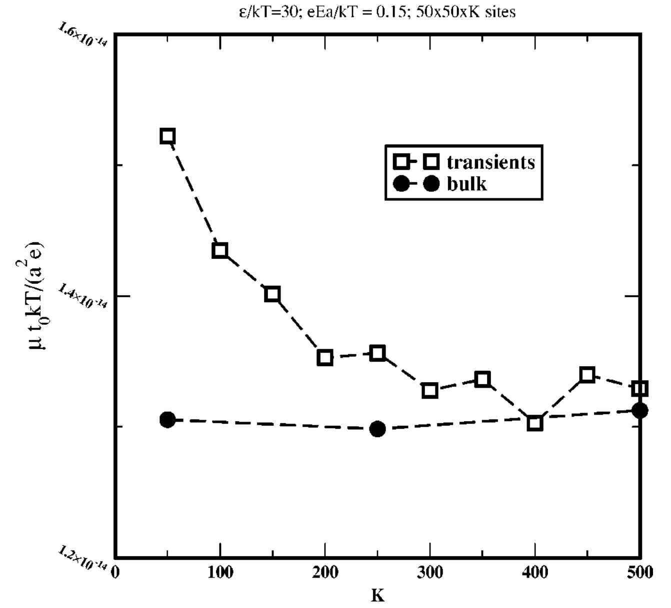

FIG. 3. Mobilities from MTRW simulations of transients (black circles) and in the bulk (open circles) transport model (see text) for the case of one trap energy. K is the number of sites in the field direction.

with all sites having the same energy (single trap energy case). Results, in reduced units, are shown in Fig. 2. The simulations were performed on a lattice of $28\times28\times28$ sites and spanned a total simulation time of $5\times10^6\tau$, τ being the average detrapping time given by Eq. (4). The time window is set equal to $5\times10^4\tau$. This is seen to be enough to extract good statistics from the random-walk simulation. The results prove that the code properly describes the transport of charge when this occurs by thermally activated detrapping.

We are also interested in proving that the code produces true *bulk*, size-independent mobilities and conductivities. In order to demonstrate this and make contact with previous papers on transient currents[10,11,17,18] we have prepared a version of the code where the calculation resembles a ''time-of-flight'' experiment. Thus, no periodic boundary conditions are applied in the direction of the field. Carriers are introduced through one border of the system (the injecting electrode) and registered at the opposite end (the collecting electrode). The transient currents are then obtained as averages over independent simulations (different realizations of the DOLS). In contrast to the bulk version of the code, the size of the sample is limited by the distance between the injecting and the collecting electrodes. The mobilities are then calculated as

$$\mu=\frac{l_{\text{sample}}}{t_r E}, \tag{6}$$

where l_{sample} is the width of the simulation cell (distance between the injecting and the collecting electrodes) and t_r is the *transient time*, that is, the time needed for the carriers to travel the distance between the two electrodes, on average.[26]

With this ''size-limited'' version of the code, we have carried out one-particle MTRW simulations of transient currents through a system with a unique site energy, as above. We considered several sample widths in the x direction (from 50 to 500 sites) and compared the results (see Fig. 3) with bulk simulations for the same sample sizes. Our calculations demonstrate that the mobilities drawn from the bulk simulation are independent of the size of the simulation cell in the x direction. That means, the bulk model corresponds to the infinite-width limit of the transient-current model. Or, in other words, that the bulk version of the code provides true *local*, size-independent, conducting properties. In a previous paper[33] this was achieved by making the system size in the field direction very large. In contrast, the application of periodic boundary conditions in the field direction for small samples leads to the same outcome. The present method allows the use of small system sizes to predict the bulk mobility of the carriers, which can be used subsequently in any macroscopic calculations based on the continuity equation[15] or on the space-charge limited conduction model.[8]

In this paper we have considered, as a standard, a DOLS of the exponential type. This has the general form

$$g(E)=\frac{N_t}{kT_0}e^{-\varepsilon/kT_0}, \tag{7}$$

where ε is the activation energy (definite positive), T_0 is a characteristic temperature that defines the *depth* of the distribution, and N_t is the total density of traps ($N_t=1/a^3$). Using this DOLS with Eq. (4) leads to a power law for the detrapping times where the governing parameter is[17,26]

$$\alpha=\frac{T}{T_0}. \tag{8}$$

D. Trap-filling effects

Our simulation method makes it possible to investigate the density dependence of the mobility for a fixed density of traps. The mobility is determined by the occupancy of the traps, which produces an enhancement of the net mobility of the carriers when their number is increased.

To describe the effect of the occupancy of the traps on the conductivity, we start from a formula for the conductivity of the Kubo-Greenwood type that relates σ to the DOLS $g(\varepsilon)$, the energy-dependent mobility $\mu(\varepsilon)$, and the probability $f(\varepsilon)$ of a trap of energy ε being occupied,[30]

$$\sigma = e\int_0^\infty g(\varepsilon)\mu(\varepsilon)f(\varepsilon)d\varepsilon. \tag{9}$$

As shown in Eq. (2), for thermally assisted transport, μ is expected to be of the form $\mu=\mu_0\exp(-\varepsilon/kT)$. For the case of a single site energy, $g(\varepsilon)=N_t\delta(\varepsilon-\varepsilon_0)$, Eq. (9) reduces to

$$\sigma = e\mu_0 N_t\int_0^\infty \delta(\varepsilon-\varepsilon_0)e^{-\varepsilon/kT}f(\varepsilon)d\varepsilon = e\mu_0 e^{-\varepsilon_0/kT}\rho, \tag{10}$$

where ρ is the number density of carriers and μ_0 is given by Eq. (3). If we have a distribution of trap energies, as shown in Fig. 1, the MTRW method reproduces a Fermi-Dirac function for the occupancy, i.e., $f(\varepsilon)=\{1+\exp[-(\varepsilon-\varepsilon_F)/kT]\}^{-1}$, with a well-defined *quasi-Fermi level* ε_F. We rewrite Eq. (9) as

$$\sigma = e\mu_0 e^{-\varepsilon_F/kT}\int_0^\infty g(\varepsilon)\left[\frac{e^{-\varepsilon/kT}}{e^{-\varepsilon_F/kT}+e^{-\varepsilon/kT}}\right]d\varepsilon \tag{11}$$

and consider the particular case where the Fermi level lies well below the conduction band, for which the term in brackets tends to 1, leaving

$$\sigma = e\mu_0 N_t e^{-\varepsilon_F/kT}. \tag{12}$$

Due to the trap-filling effect, the quasi-Fermi level is a monotonically increasing function of the density of carriers. See, for instance, Fig. 1. In order to estimate quantitatively this effect, we start with the definition of the carrier density in terms of the DOLS, and expand about $\varepsilon=\varepsilon_F$ after integrating by parts (see Appendix A),

$$\rho = \int_0^\infty g(\varepsilon)f(\varepsilon)d\varepsilon \sim \int_{\varepsilon_F}^\infty g(\varepsilon)d\varepsilon - (1/6) \times(\pi k_B T)^2 d^2\left\{\int_\varepsilon^\infty g(\varepsilon)d\varepsilon\right\}\Big/ d\varepsilon^2\Big)_{\varepsilon=\varepsilon_F} + \cdots. \tag{13a}$$

We now focus on the exponential DOLS of Eq. (7). We have then

$$\rho \sim \int_{\varepsilon_F}^\infty \frac{N_t}{kT_0}e^{-\varepsilon/kT_0}d\varepsilon + (N_t/6)\pi^2(T/T_0)^2\exp(-\varepsilon_F/kT_0) + \cdots, \tag{13b}$$

which leads to fourth order in α to (see Appendix A),

$$\varepsilon_F = -kT_0\ln\left(\frac{\rho}{N_t[1+(\pi\alpha)^2/6+7(\pi\alpha)^4/360]}\right). \tag{13c}$$

By inserting Eq. (13c) in Eq. (12) we obtain

$$\sigma = e\mu_0 N_t e^{-\varepsilon_F/kT} = e\mu_0 N_t\left(\frac{\rho}{N_t[1+(\pi\alpha)^2/6+7(\pi\alpha)^4/360]}\right)^{1/\alpha}, \tag{13d}$$

which predicts a power-law dependence for the conductivity on carrier density of exponent $1/\alpha, \alpha=T/T_0$. For the exponential DOLS, higher terms in Eq. (13b) do not change this power-law form.

For small α, or when the Fermi level is deep enough at a finite temperature, we will have

$$\varepsilon_F = -kT_0\ln\left(\frac{\rho}{N_t}\right) \tag{14}$$

and

$$\sigma = e\rho_c\mu_0 = e\mu_0 N_t\left(\frac{\rho}{N_t}\right)^{1/\alpha} \tag{15}$$

with ρ_c representing the average density of carriers in the conduction band.

In Table I and Figs. 1 and 4 we present results from MTRW simulations with an exponential DOLS at three-different densities of carriers. All simulations were performed with a fixed number of ten particles. The size of system is N^3, with N set to 28, 24, and 18, respectively. Also we introduce an energy cutoff of 0.8 eV in order to limit the CPU time required to carry out the simulation. For the DOLS and densities considered here the effect of the cutoff on the results is very small. The results were obtained after averaging over 50–100 realizations of the DOLS and with a time window of 0.01 τ, τ being the maximum detrapping time for each realization. The applied field in all cases was 3×10^5 V m^{-1}

As shown in Fig. 1, the simulation leads to a well-defined Fermi level. In Table I we compare these Fermi energies with the predictions of Eqs. (14) and (13c) and show that this last equation reproduces the Fermi energies obtained in the simulation to well within statistical errors, whereas Eq. (14) is only partially fulfilled at the smallest α. The fact that ε_F obeys a logarithmic law in all cases explains the power law of exponent $1/\alpha$ for the conductivity. We observe that Eq. (11) used with the trap occupancy distributions predicted by the simulation reproduces the conductivities yielded by the MTRW simulation. The approximations, Eqs. (13d) and (15), only match the simulation for progressively larger α's, for which the Fermi level lies well below the conduction band.

We note that this description in terms of Fermi-Dirac statistics is not expected to be valid in the limit of strong recombination, in which case the assumption of thermodynamic equilibrium between traps and conduction band breaks

TABLE I. Conductivities and Fermi levels for exponential DOLS as obtained from MTRW simulations and theoretical predictions (see text).

			Log σ $(\Omega\,\mathrm{m})^{-1}$				ε_F (eV)		
α	Particles/sites	ρ (m^{-3})	MTRW	Eq. (11)	Eq. (15)	Eq. (13d)	MTRW	Eq. (14)	Eq. (13c)
	$10/28^3$	5.69×10^{22}	−1.30	−1.36	−0.33	−0.99	0.259	0.199	0.237
1	$10/24^3$	9.04×10^{22}	−1.06	−1.13	−0.13	−0.78	0.245	0.187	0.225
	$10/18^3$	2.14×10^{23}	−0.65	−0.70	0.25	−0.41	0.219	0.165	0.203
	$10/28^3$	5.69×10^{22}	−3.97	−3.90	−3.67	−4.04	0.425	0.397	0.417
0.5	$10/24^3$	9.04×10^{22}	−3.62	−3.67	−3.27	−3.64	0.398	0.374	0.394
	$10/18^3$	2.14×10^{23}	−2.85	−2.94	−2.52	−2.84	0.355	0.329	0.349
	$10/28^3$	5.69×10^{22}	−7.61	−7.88	−7.77	−7.91	0.648	0.637	0.646
0.3125	$10/24^3$	9.04×10^{22}	−7.07	−7.31	−7.12	−7.27	0.615	0.598	0.608
	$10/18^3$	2.14×10^{23}	−5.92	−6.12	−5.91	−6.07	0.544	0.527	0.536

down. In this section our objective is to demonstrate that for the cases studied, the simulation results can be described in terms of Fermi-Dirac distributions and quasi-Fermi levels. The general simulation procedure is quite capable of describing more complicated cases, such as those in which recombination is the determining factor.

III. APPLICATION TO SENSITIZED TiO_2

In this section we apply our method to the case of sensitized nanocrystalline TiO_2, which provides a model system for the study of pure electron transport between traps. There is experimental evidence[15,4,13,34,35] that electron transport in this system exhibits nonlinear behavior which is usually explained in terms of trap-filling effects.

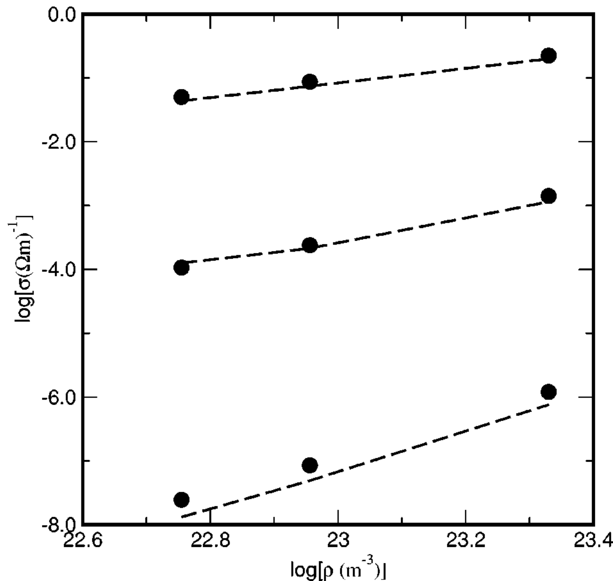

FIG. 4. Illustration of the trap-filing effect: the conductivity increases linearly or superlinearly with the density of carriers in the MTRW simulations. The plot is double logarithmic with the dashed lines corresponding to the predictions of Eq. (11). Logσ follows a straight line of approximate slope $1/\alpha$, where α is given by Eq. (8). Cases shown are for $\alpha=1$, 0.5, and 0.3125 (from top to bottom). See Table I for details.

Our results described above indicate that dispersive transport with trap filling leads to a conductivity that is nonlinear with ρ, varying as

$$\sigma\propto\rho^{1/\alpha} \tag{16}$$

in the special case of an exponential DOLS with characteristic parameter α. Although the dependence of σ on ρ is not easy to observe experimentally, the dependence of σ on light intensity can be readily measured. For sensitized nanocrystalline TiO_2, it has been found[4] that the dc photoconductivity has a power-law dependence with respect to the degree of illumination (i.e., the volume photogeneration rate G) of the form

$$\sigma\propto G^{\beta}, \tag{17}$$

where β is around 1.6.[4,15] This could result from the dependence of σ on ρ, if certain assumptions are made about carrier recombination (discussed below).

To relate the density of carriers to the degree of illumination, we assume that, in the stationary state, the volume photogeneration rate G equals the recombination rate R. Thus,

$$G=R=\rho/\tau, \tag{18}$$

where τ is the lifetime of the electrons that is, in general, carrier density dependent. Equations (16), (17), and (18) imply that the lifetime obeys another power law with respect to the degree of illumination

$$\tau\propto G^{-\gamma}, \tag{19}$$

where

$$\gamma=1-\alpha\beta. \tag{20}$$

A power-law variation of τ with G has been observed in both electrolyte-supported and dry TiO_2 films[14,15,36,37] for which γ lies in the range 0.5 ± 0.2. The exponent is a function of the chemical environment and it is not known exactly how τ depends on G for the system of Ref. 4. For our current purpose we will assume $\gamma=0.5$. Using a different dependence would change the shape of the DOLS needed to reproduce the experimental behavior, but it would not change the quali-

tative result, i.e., that trap filling can explain the superlinear dependence of photoconductivity on light intensity.

Assuming $\gamma = 0.5$ and $\beta = 1.6$, we get $\alpha = 0.31$ as the characteristic parameter of the exponential DOLS. This value is in good agreement with that used to reproduce transient experiments in TiO_2 electrodes[17] ($\alpha = 0.37$) as well as with recent studies[16] on electron transport in nanoporous TiO_2. It also implies that, according to Eq. (16), the photoconductivity has an almost *cubic* dependence on the density; this is a strong evidence of trap filling.

We have simulated sensitized TiO_2 at 300 K using the MTRW code for several DOLS at three different steady-state electron densities. These have been estimated from the experimental degrees of illumination[4] and the known behavior of the lifetime vs the photogeneration rate (see Appendix B). We use an average distance between traps of $a = 20$ Å, extracted from the quoted densities of traps on the surface of the nanoparticulates[38] and nanoparticle radius (about 10 nm). Also, we take the applied field to be 3×10^5 V m^{-1}. This has only a very small influence on the detrapping times as calculated by Eq. (4). We set the time-window to be 0.1 τ (τ is the maximum detrapping time for each realization of the DOLS). The current density was obtained from averaging over 50 time-windows once the steady state for each realization was achieved. Simulations were performed with ten particles in all cases and a system size of N^3, N being 28, 24, and 18 for the three densities studied, respectively. The time scale was fixed by setting $t_0 = 5 \times 10^{-13}$ s. This value has been shown to be adequate to describe transient currents with the random-walk model in the *absence of recombination*.[17] Nevertheless, the choice of t_0 does not affect the density dependence of the photoconductivity, rather it introduces a constant shift that can be corrected once more precise data for phonon frequencies in nanocrystal TiO_2 are available.

We have used an exponential DOLS with $\alpha = 0.31$. This is a deep distribution, there is a non-negligible number of traps with a high activation energy and very long residence times. This requires a large time-window to correctly sample the DOLS. Nevertheless, traps with very long residence times are not likely to contribute to the conductivity as these times are longer than the lifetimes of the electrons in the material (see Appendix B). In other words: electrons will recombine long before they detrap to a neighboring trap. Based on this, we have introduced a cutoff of 1.0 eV in the DOLS. This cutoff will have an effect on the numerical results. The effect is small at the densities considered here but could be large at much lower densities.[29] In the present paper the choice of cutoff is an integral part of the model. This keeps the computational cost within reasonable limits (around 12 h on a PC of 400 MHz). As it can be seen in Fig. 6, the conductivities still follow a power law, although the slope in the double-logarithmic plot is slightly larger than $1/\alpha$.

As an alternative to the exponential DOLS, we have tried more realistic distributions based on spectroscopic and adsorption measurements. Göpel, Rocker, and Feierabend[39] have performed an extensive study of the (110) surface of rutile TiO_2 (the most stable surface of the rutile phase of this oxide). These authors report two kinds of surface intraband defect states located at 0.32 and 0.51 eV below the conduction-band edge, respectively. The former corresponds to oxygen vacancies in the oxide surface, whereas the second are associated with the first ionization state of these vacancies. Bearing this in mind, we have constructed a DOLS where 0.32 eV traps are predominant, but where there are also a few 0.50-eV traps. This has been modeled by means of Gaussians (see Fig. 5) centered at 0.32 and 0.5 eV, respectively, with widths σ_ε and weights A's used as adjustable parameters,

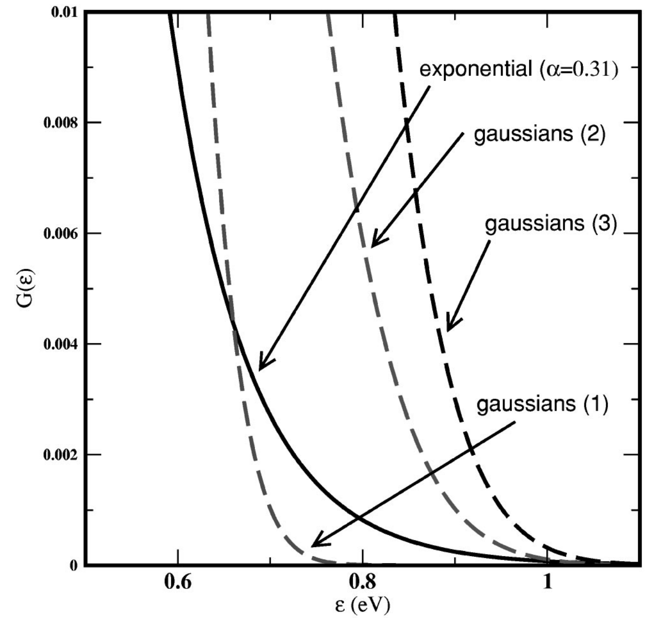

FIG. 5. DOLS used in this paper to describe electron transport in sensitized TiO_2. The Gaussian distributions are obtained from Eq. (21) with $A_1 = 0.99$, $A_2 = 0.01$, $\sigma_{\varepsilon 1} = 0.1$ eV, and $\sigma_{\varepsilon 2} = 0.1$ eV for case (1), $A_1 = 0.99$, $A_2 = 0.01$, $\sigma_{\varepsilon 1} = 0.01$ eV, and $\sigma_{\varepsilon 2} = 0.2$ eV for case (2) and $A_1 = 0.97$, $A_2 = 0.03$, $\sigma_{\varepsilon 1} = 0.1$ eV, and $\sigma_{\varepsilon 2} = 0.2$ eV for case (3). To highlight the difference between all distributions, only the region of very deep traps is shown in the figure.

$$g(\varepsilon) = A_1 \exp[-(\varepsilon - 0.32)^2/\sigma_{\varepsilon 1}^2] + A_2 \exp[-(\varepsilon - 0.5)^2/\sigma_{\varepsilon 2}^2]. \tag{21}$$

In Fig. 6 the photoconductivities obtained for DOLS describing sensitized TiO_2 are plotted versus the light intensity. It can be seen that both an exponential DOLS and the Gaussians for which the dispersion of values around the mean value for the deeper trap of 0.5 eV is 0.2 eV give the correct slope with respect to the experiment. A smaller dispersion (i.e., 0.1 eV) does not lead to the correct slope for the Gaussian model. This implies that it is the very small proportion (1%) of deep traps that control the conductivity. In addition, for the t_0 parameter chosen above, it is observed that the simulation provides photoconductivities of the order of the experiment, provided the DOLS is composed of 97% traps of energy 0.32 ± 0.1 eV and 3% of 0.5 ± 0.2 eV. Thus, it is the parameter $\sigma_{\varepsilon 2}$ (tuning the *tail* of the DOLS) that determines the *slope* in the conductivity-illumination curve whereas the

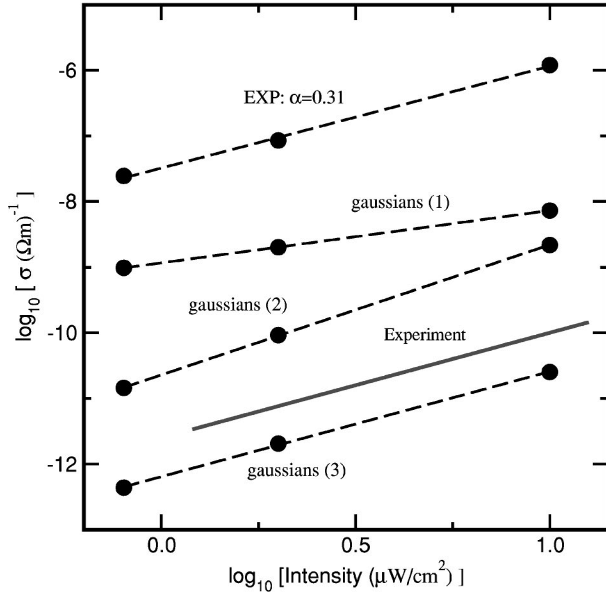

FIG. 6. Photoconductivities vs illumination intensity in sensitized TiO_2 from MTRW simulations for the DOLS of Fig. 6. The dashed lines correspond to linear fits of the simulation points. Experimental data are taken from Ref. 4.

parameter A_2 (giving the overall *proportion* of deep traps) controls the magnitude of the photoconductivity.

IV. CONCLUSIONS

In this paper we have devised a simulation code based on a multiple-trapping model of charge transport, which can predict local (or microscopic) conducting properties in disordered materials. We have tested the model against limiting cases (single trap energy and an exponential density of states) for which we have derived analytic results for conductivities and Fermi levels. The model and its corresponding code have been shown to reproduce true *bulk* conducting properties and to demonstrate trap-filling effects, known to be relevant to many experimental systems. We have considered a very simple model mechanism of conduction that involves thermal excitation from traps, with neglect of direct tunneling from trap to trap or scattering processes in the conduction band. We show that this choice is plausible for systems with a large dispersion of trap energies. In addition, we have shown that the MTRW simulation in the steady state obeys Fermi-Dirac statistics with a Fermi level that is a monotonically increasing function of the density of carriers.

For TiO_2 we have seen that it is possible to construct a reasonable DOLS that gives rise to the observed illumination dependence of the photoconductivity. We have also proved that it is the relatively small region of very deep traps that control the magnitude and the slope of the conductivity–light intensity curve. Thus, it is necessary to include in the model a sufficient amount of very deep traps to obtain an enhancement of the mobility at high injection levels. Clearly, more information about deep traps is vital if the model is to be improved.

At present the simulation does not take into account recombination in an explicit way. Work is in progress to introduce recombination (and generation) explicitly in the code and provide a fuller microscopic description of photoconduction.

ACKNOWLEDGMENTS

J.A.A. has been supported by Electricité de France. J.N. acknowledges support from Greenpeace Environmental Trust and EPSRC. N.Q. thanks EPSRC for computational facilities awarded under Grant No. GR/M94427.

APPENDIX A: DERIVATION OF Eq. (13c)

We define the function

$$\Gamma(\varepsilon)=\int_0^{\varepsilon} g(\varepsilon)d\varepsilon \tag{A1}$$

and rewrite Eq. (13a) as

$$\rho=\int_0^{\infty} g(\varepsilon)f(\varepsilon)d\varepsilon=\int_{-\infty}^{\infty} f(\varepsilon)\frac{d\Gamma}{d\varepsilon}d\varepsilon, \tag{A2}$$

which can be integrated by parts to give

$$\rho=f(\varepsilon)\Gamma(\varepsilon)|_{-\infty}^{\infty}-\int_{-\infty}^{\infty}\Gamma(\varepsilon)df=\Gamma(\infty)-\int_{-\infty}^{\infty}\Gamma(\varepsilon)df. \tag{A3}$$

We now formulate a Taylor expansion of $\Gamma(\varepsilon)$ about ε_F and write

$$\rho=\Gamma(\infty)-\Gamma(\varepsilon_F)\int_{-\infty}^{\infty}df+\left.\frac{d\Gamma}{d\varepsilon}\right|_{\varepsilon_F}\int_{-\infty}^{\infty}(\varepsilon-\varepsilon_F)df+\frac{1}{2}\left.\frac{d^2\Gamma}{d\varepsilon^2}\right|_{\varepsilon_F}\int_{-\infty}^{\infty}(\varepsilon-\varepsilon_F)^2df+\frac{1}{3!}\left.\frac{d^3\Gamma}{d\varepsilon^3}\right|_{\varepsilon_F}\int_{-\infty}^{\infty}(\varepsilon-\varepsilon_F)^3df+\frac{1}{4!}\left.\frac{d^4\Gamma}{d\varepsilon^4}\right|_{\varepsilon_F}\int_{-\infty}^{\infty}(\varepsilon-\varepsilon_F)^4df+\cdots. \tag{A4}$$

Odd terms in $(\varepsilon-\varepsilon_F)$ integrate to zero,

$$\int_{-\infty}^{\infty}\frac{x^n\exp(x)}{[1+\exp(x)]^2}dx=0 \quad (\text{for } n \text{ odd}), \tag{A5}$$

whereas

$$\int_{-\infty}^{\infty}\frac{x^2\exp(x)}{[1+\exp(x)]^2}dx=\pi^2/3,$$

$$\int_{-\infty}^{\infty}\frac{x^4\exp(x)}{[1+\exp(x)]^2}dx=7\pi^4/15, \tag{A6}$$

where $x=(\varepsilon-\varepsilon_F)/kT$. On the other hand,

TABLE II. Volume generation rates, lifetimes and steady-state electron densities for PbS-sensitized TiO_2 1 μm films.

I (μW/cm^2)	G (m^{-3} s^{-1})	J_{ph} (A m^{-2})	τ (s)	ρ (m^{-3})
0.8	9.79×10^{20}	2.8×10^{-5}	59.76	5.85×10^{22}
2.0	2.45×10^{21}	7.0×10^{-5}	37.79	9.25×10^{22}
10.0	1.22×10^{22}	3.5×10^{-4}	16.90	2.07×10^{23}

$$\frac{d^2\Gamma}{d\varepsilon^2}=\frac{-N_T}{(kT_0)^2}\exp(-\varepsilon/kT_0),$$

$$\frac{d^4\Gamma}{d\varepsilon^4}=\frac{-N_T}{(kT_0)^4}\exp(-\varepsilon/kT_0). \tag{A7}$$

By inserting Eqs. (A5), (A6), and (A7) into Eq. (A4), we get

$$\begin{aligned}\rho&=\int_{\varepsilon_F}^{\infty}g(\varepsilon)d\varepsilon+N_T\frac{\pi^2}{6}\alpha^2\exp(-\varepsilon_F/kT_0)\\&\quad+N_T\frac{7\pi^4}{360}\alpha^4\exp(-\varepsilon_F/kT_0)+\cdots\\&=N_T\exp(-\varepsilon_F/kT_0)\left(1+\frac{\pi^2}{6}\alpha^2+\frac{7\pi^4}{360}\alpha^4+\cdots\right),\end{aligned} \tag{A8}$$

hence

$$\varepsilon_F=-kT_0\ln\left(\frac{\rho}{N_1[1+(\pi\alpha)^2/6+7(\pi\alpha)^4/360]+\cdots}\right). \tag{A9}$$

APPENDIX B: CALCULATION OF STEADY-STATE ELECTRON DENSITIES

To obtain electron densities in TiO_2 electrodes under steady-state illumination, we start from the following expression for the volume generation rate

$$G=(1-r)(1-e^{\alpha_a d})\frac{I}{E_{ph}}d^{-1}, \tag{B1}$$

where r is the fraction of light lost by scattering, reflection, and absorption in outer layers, α_a is the light absorption coefficient, I is the light intensity, E_{ph} the energy of a photon, and d is the thickness of the film.

The average lifetime of the electrons is related to the photoinduced current density via[15]

$$\tau=\tau_0 j_{ph}{}^{-\gamma}. \tag{B2}$$

The photoinduced current density is in turn related to the light intensity through the photoresponse P. This quantity is defined by the ratio between current intensity and light intensity, i.e.,

$$j_{ph}=\frac{PI}{ld}, \tag{B3}$$

where l is the separation of the electrodes. Once the lifetime and the generation rate are known, the number density of electrons is obtained from Eq. (21).

We have focused on the case studied in Ref. 4. In this paper, the photoconductivity of porous TiO_2 films sensitized with PbS is measured under several degrees of illumination ranging from 0.8 to 10 μW/cm^2. The thickness of the films is 1 μm and a voltage of 100 V is applied between two electrodes separated 300 μm. For these films, the photoresponse measured at 500 nm is 35×10^{-12} A W^{-1} m^2.

In order to obtain the volume generation rate from Eq. (B1) we need to know the absorption coefficient of PbS-sensitized TiO_2 at 500 nm and the fraction R. We have taken $\alpha_a=7.2\times 10^4$ m^{-1} from a comparison of data in Ref. 4 with the measured absorption coefficient of unsensitized TiO_2 and $r=0.3$.[40] The volume generation rates obtained from these data are shown in Table II.

[1] L. A. Dissado and J. C. Fothergill, *Electrical Degradation and Breakdown in Polymers* (Peter Peregrinus, London, 1992).
[2] J. J. O'Dwyer, *The Theory of Electrical Conduction and Breakdown in Solid Dielectrics* (Clarendon, Oxford, 1973).
[3] E. A. Meulenkamp, J. Phys. Chem. B **103**, 7831 (1999).
[4] P. Hoyer and R. Könenkamp, Appl. Phys. Lett. **66**, 349 (1995).
[5] B. O'Regan and M. Grätzel, Nature (London) **353**, 737 (1991).
[6] Laboratory for Photonics and Interfaces, Lausanne, Switzerland, http://dcwww.epfl.ch/lpi/solarcellE.html
[7] S. A. Haque, Y. Tachibana, R. L. Willis, J. E. Moser, M. Grätzel, D. R. Klug, and J. R. Durrant, J. Phys. Chem. B **104**, 538 (2000).
[8] P. W. M. Blom, M. J. M. de Jong, and M. G. van Munster, Phys. Rev. B **55**, R656 (1997).
[9] A. J. Campbell *et al.*, J. Appl. Phys. **84**, 6737 (1998).
[10] G. Schönherr, H. Bässler, and M. Silver, Philos. Mag. B **44**, 47 (1981).
[11] P. M. Borsenberger, L. Pautmeier, and H. Bässler, J. Chem. Phys. **94**, 5447 (1991).
[12] R. A. Street, *Hydrogenated Disordered Silicon* (Cambridge University Press, Cambridge, UK, 1991).
[13] P. E. de Jongh and D. Vanmaekelbergh, Phys. Rev. Lett. **77**, 3427 (1996).
[14] L. M. Peter, E. A. Ponomarev, G. Franco, and N. J. Shaw, Electrochim. Acta **45**, 549 (1998).
[15] L. M. Peter and K. G. U. Wijayantha, Electrochem. Commun. **1**, 576 (1999).
[16] R. Könenkamp, Phys. Rev. B **61**, 11 057 (2000).

[17] J. Nelson, Phys. Rev. B **59**, 15 374 (1999).
[18] A. Jakobs and K. Kehr, Phys. Rev. B **48**, 8780 (1993); P. Argyrakis, A. Milchev, V. Pereyra, and K. W. Kehr, Phys. Rev. E **52**, 3623 (1995); B. Hartenstein, H. Bassler, A. Jacobs, and K. W. Kehr, Phys. Rev. B **54**, 8574 (1996).
[19] F. W. Schmidlin, Phys. Rev. B **16**, 2362 (1977).
[20] For example, K. W. Kehr, K. Mussawisade, T. Wichmann, and W. Dieterich, Phys. Rev. E **56**, 2351 (1997); K. W. Kehr, K. Mussawisade, T. Wichmann, and W. Dieterich, Phys. Status Solidi B **205**, 73 (1998).
[21] Y. Chen, Y. Cao, Y. Bai, W. Yang, J. Yang, H. Jin, and T. Li, J. Vac. Sci. Technol. B **15**, 1442 (1997).
[22] P. J. D. Lindan, N. M. Harrison, M. J. Gillan, and J. A. White, Phys. Rev. B **55**, 15 919 (1997).
[23] This would correspond to the coordination number of the lattice in the case that we consider jumps between nearest neighbors only. Thus, for a simple cubic: $l=6$.
[24] H. J. Wintle, IEEE Trans. Dielectr. Electr. Insul. **6**, 1 (1999).
[25] J. M. Marshall, Philos. Mag. B **38**, 335 (1978).
[26] H. Scher and E. W. Montroll, Phys. Rev. B **12**, 2455 (1975).
[27] See, for example, C. Garrod, *Statistical Mechanics and Thermodynamics* (Oxford University Press, 1995), p. 219.
[28] J. Nelson, S. A. Haque, D. R. Klug, and J. R. Durrant, Phys. Rev. B **63**, 205321 (2001).
[29] J. A. Anta, G. Marcelli, M. Meunier, and N. Quirke (unpublished).
[30] P. Nagels, *Electronic Transport in Disordered Semiconductors*, Chapter 5 in Amorphous Semiconductors, topics in Applied Physics, Vol. 36, edited by M. H. Brodsky (Springer-Verlag, Berlin, 1979).
[31] G. Pfister and H. Scher, Adv. Phys. **27**, 747 (1978).
[32] M. Silver and L. Cohen, Phys. Rev. B **15**, 3276 (1977).
[33] S. V. Novikov, D. H. Dunlap, V. M. Kenkre, P. E. Parris, and A. V. Vannikov, Phys. Rev. Lett. **81**, 4472 (1998).
[34] K. Schwarzburg and F. Willig, Appl. Phys. Lett. **58**, 2520 (1991).
[35] F. Cao, G. Oskam, P. C. Searson, J. M. Stipkala, T. A. Heimer, F. Farzad, and G. J. Meyer, J. Phys. Chem. **99**, 11 974 (1995).
[36] R. Könenkamp and R. Henninger, Appl. Phys. A: Solids Surf. **58**, 87 (1994).
[37] G. Schlichthörl, N. G. Park, and A. J. Frank, J. Phys. Chem. B **103**, 782 (1999).
[38] G. Rothenberger, D. Fitzmaurice, and M. Grätzel, J. Phys. Chem. **96**, 5552 (1994).
[39] W. Göpel, G. Rocker, and R. Feierabend, Phys. Rev. B **28**, 3427 (1983).
[40] W. Shockley and W. T. Read, Jr., Phys. Rev. **87**, 835 (1952).